Trans. Phenom. Nano Micro Scales, 8(1): 32-38, Winter and Spring 2020
DOI: 10.22111/tpnms.2019.22515.1135

ORIGINAL RESEARCH PAPER

Analytical Spring-Mass Model of Impact Behavior of Double-Walled Carbon Nanotubes

Sajjad Seifoori[1,], Fatemeh Abbaspour[2] , Ehsan Zamani[2]*

[1]*Mechanical Engineering Dept., Faculty of Engineering, Vali-e-Asr University of Rafsanjan, Iran*
[2]*Mechanical Engineering Dept., Faculty of Engineering, Shahrekord University, Shahrekord, Iran*

Received 30 October 2017; revised 17 December 2019; accepted 19 December 2019; available online 22 February 2020

ABSTRACT: In this study, an impact behavior of spherical striker on a double-walled carbon nanotube (DWCNT) is presented based on a three degree of freedom spring-mass model and the finite element (FE) simulations. The semi-analytical solution of the transverse impact of a striker on a DWCNT is investigated by using the elasticity nonlocal theory of Euler-Bernoulli (EBT) and Timoshenko (TBT) nanobeams. The spring-mass system with spring constant is used that involves shear and bending deformation. The van der Waals (vdW) interaction between two layers of a DWCNT is included in the analytical model. The results of this analysis are compared with the results of the FE simulation. The results from the spring-mass model demonstrated good agreement with FE simulation for various values of a DWCNT dimension, chirality, boundary condition, number of layered and also striker parameters such as mass and velocity. The DWCNT independent of vdW interaction is more flexible than DWCNT with vdW forces.

KEYWORDS: *Double-Walled Carbon Nanotube; FE simulation; Impact; spring-mass system*

INTRODUCTION

The Development of applicable analytical models to predict the behavior of nanobeam under dynamic loading is an important subject concerning the application of nanostructures. Because of the nonlocal elasticity theory proposed by Eringen [1–3], the stress state at a particular point in the continuum, is dependent on strain states at all points on the solid.

A lot of research has been done to study the mechanical behavior of carbon nanotubes. Seifoori et al. [4-5] presented the nonlocal Single-Walled Carbon Nanotube theory for both EBT and TBT nanobeam. Reddy [6-7] derived the equations of motion of the beams by nonlocal theory. Analytical solutions of bending, vibration, and buckling were presented to bring out the effect of the nonlocal behavior by using the nonlocal theories. Simsek [8] presented an analytical method for the forced vibration of an elastically connected double-carbon nanotube system (DWCNTS) carrying a moving nanoparticle based on the nonlocal elasticity theory. Seifoori and Liaghat [9] formulated the nonlocal model of the Timoshenko (TBT) beam theory and developed an analytical solution of the impact of a mass on simply supported and clamped nanobeams. An improved 3D explicit finite element model for armchair and zigzag SWNTs was developed. Seifoori [10], also investigated the dynamics of the impact of a nano particle on carbon nanotubes based on two degrees of freedom model. Modeling the van der Waals (vdW) interaction is an important step in the continuum modeling of a multi-walled nanotube.

Along with these models, most usual one is the Winkler type foundation model for vdW forces. Pradhan and Phadikar [11] studied stiffness of the Winkler foundation of the nanoplate on vibration frequencies. Interaction between the vdW force and the nonlocal parameter was investigated. In this paper, the impact of spherical striker on DWCNT is investigated by an analytical model and then results are compared with the FEM simulation. FE simulations for estimating dynamic behavior of DWCNT are done to illustrate the accuracy of this analytical technique. Based on these simulations, the maximum dynamic deflections of DWCNT with different geometries as well as striker mass and velocity are obtained and then compared with theory investigation.

THE ANALYTICAL MODEL

The governing equations for double-walled Euler–Bernoulli and Timoshenko beam (nanotube) theory model in terms of the transverse displacement can be obtained as [11] based on the nonlocal

$$H\frac{\partial^4 z_1}{\partial x^4} + k(z_1 - z_2) - k\mu\left(\frac{\partial^2 z_1}{\partial x^2} - \frac{\partial^2 z_2}{\partial x^2}\right) + B\frac{\partial^2 z_1}{\partial t^2} - B\mu\left(\frac{\partial^4 z_1}{\partial x^2 \partial t^2}\right) - q + \mu\frac{\partial^2 q}{\partial x^2} = 0 \quad (1)$$

✉ *Corresponding Author Email: *sajjad.seifoori@vru.ac.ir*
Tel.: +989124304396; Note. This manuscript was submitted on October 30, 2017; approved on December 19, 2019; published online February 22, 2020.

Nomenclature

A_1	Cross section area for outer nanotube	L	length the beam
A_2	Cross section area for inner nanotube	m_1	Striker mass
d	Outside nanotube diameter	m_2	Inner nanotube mass
E	Young's modulus of the material	m_3	Outer nanotube mass
G	shear modulus of the material	P_{12}	Van der Waals force
I_1	Moment of inertia for outer nanotube	R	Radius of spherical striker
I_2	Moment of inertia for inner nanotube	V_0	Impact velocity
k_1	Spring stiffness for outer nanotube	$z_{1,2,3}$	Vertical displacement
k_2	Spring stiffness for inner nanotube		**Greek Symbols**
k_c	Contact Spring stiffness	μ	nonlocal parameter
k_s	shear correction factor	ν	Poisson's ratio
k_v	Van der Waals interaction stiffness	ρ	density

$$H\frac{\partial^4 z_2}{\partial x^4}+k(z_2-z_1)-k\mu\left(\frac{\partial^2 Zz_2}{\partial x^2}-\frac{\partial^2 z}{\partial x^2}\right) +B\frac{\partial^2 z_2}{\partial t^2}-B\mu\left(\frac{\partial^4 z_2}{\partial x^2\partial t^2}\right)=0 \quad (2)$$

Where $B=\rho A$ and $H=EI$.

$$J_1\left(\frac{\partial^2 z_1}{\partial x^2}-\frac{\partial \varphi_1}{\partial x}\right)+\left[P_{12}-\mu\frac{\partial^2 p_{12}}{\partial x^2}\right]=B_1\frac{\partial^2}{\partial t^2}\left[z_1-\mu\frac{\partial^2 z_1}{\partial x^2}\right] \quad (3)$$

$$H_1\frac{\partial^2 \varphi_1}{\partial x^2}+J_1\left(\frac{\partial z_1}{\partial x}-\varphi_1\right)=\rho I_1\frac{\partial^2}{\partial t^2}\left[\varphi_1-\mu\frac{\partial^2 \varphi_1}{\partial x^2}\right] \quad (4)$$

$$J_2\left(\frac{\partial^2 z_2}{\partial x^2}-\frac{\partial \varphi_2}{\partial x}\right)-\left[P_{12}-\mu\frac{\partial^2 p_{12}}{\partial x^2}\right]=B_2\frac{\partial^2}{\partial t^2}\left[z_2-\mu\frac{\partial^2 z_2}{\partial x^2}\right] \quad (5)$$

$$H_2\frac{\partial^2 \varphi_2}{\partial x^2}+J_2\left(\frac{\partial z_2}{\partial x}-\varphi_2\right)=\rho I_2\frac{\partial^2}{\partial t^2}\left[\varphi_2-\mu\frac{\partial^2 \varphi_2}{\partial x^2}\right] \quad (6)$$

Where $J_1=k_sGA_1$, $J_2=k_sGA_2$, $B_1=\rho A_1$, $B_2=\rho A_2$ and $H_1=\rho A_1$, $H_2=\rho A_1$. The equations 3 and 4 are connected to the central nanotube and the equations 5 and 6 are associated with the outside nanotube. P_{12} is vdW interaction per unit length between two layers in the nanotube.

For small vibration, vdW force in any location between two layers is related to deflection between two layers (nanotubes), and can be considered as following [12];

$$P_{12}=k_v(z_1-z_2) \quad (7)$$

Where k_v is the constant of vdW force and can be considered as $k_v=\frac{320\,(2R_1)\ erg/cm^2}{0.16d^2}, d=1.42\times10^{-8}\ cm.$ Where R_1 is the radius of inside nanotube in DWCNT. According to Figure 1, the spring-mass system consists of k_1 and k_2 linear spring, k_c non-linear spring, which denoted for the contact stiffness and k_v spring constant that expresses the vdW force between two layers of nanotubes.

In Figure 1 the stiffness k_1 and k_2 are represented the linear springs (until deformation remains small) with account the geometry of the structure, the boundary conditions, bending and shear deformations.

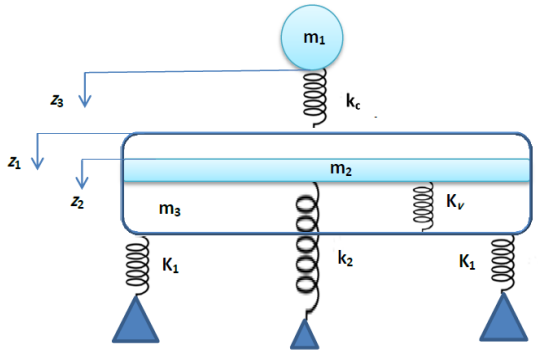


Fig. 1. The semi-analytical spring-mass model for impact on DWCNT

The contact force regime is $F=k_c(z_3-z_1)^{\frac{3}{2}}$ that z_3 is the displacement of the striker and z_1 is the displacement of the beam.

This is Hertz's contact law and applicable for both the loading and the unloading phases.

The equations of motion of the system in Figure 1 are as following,

$$m_3\ddot{z}_3+k_c(z_3-z_1)^{3/2}=0 \quad (8)$$

$$m_2\ddot{z}_1+k_2z_1-k_c(z_3-z_{12})^{3/2}+k_v(z_1-z_2)=0 \quad (9)$$

$$m_1\ddot{z}_2+k_1z_2-k_v(z_1-z_2)=0 \quad (10)$$

The system has the initial conditions as:

$$z_1(0)=0,\ \dot{z}_1(0)=0, z_2(0)=0, \dot{z}_2(0)=0, z_3(0)=0,\ \dot{z}_3(0)=V_0 \quad (11)$$

To solve the equations of this system, the change of variables are used to solve the problem. When $z_3 > z_1$ the contact force will be deleted and the equations of motion are as below:

$$m_3\ddot{z}_3 = 0 \tag{12}$$

$$m_2\ddot{z}_1 + k_2 z_1 + k_v(z_1 - z_2) = 0 \tag{13}$$

$$m_1\ddot{z}_2 + k_1 z_2 - k_v(z_1 - z_2) = 0 \tag{14}$$

Springs constants

The k_1 and k_2 value for the Euler–Bernoulli and Timoshenko nanobeam are presented by considering the static deflection for both simply supported and clamped supported boundary conditions. Due to the force-displacement relation, when force is effected in the middle of the nanotube, force expressed as $F = k\, z_E \left(\frac{L}{2}\right)$.

So k_1 and k_2 value for the simply supported EBT nanotube are represented as follows,

$$k_1 = \sum_{n=1}^{\infty} \frac{\beta_1}{\lambda_n sin^2\, \frac{n\pi}{2}} \tag{15}$$

$$k_2 = \sum_{n=1}^{\infty} \frac{\beta_2}{\lambda_n \sin^2\, \frac{n\pi}{2}} \tag{16}$$

Where $\beta_1 = \frac{EI_1 n^4\pi^4}{2L^3}$, $\beta_2 = \frac{EI_2 n^4\pi^4}{2L^3}$ and k_1 is the spring constant for inside nanotube and k_2 is the spring constant for outside nanotube. k_1 and k_2 for clamped supported EBT nanobeam are presented as,

$$k_1 = \sum_{n=1}^{\infty} \frac{8\,\beta_1}{\lambda_n \sin^2(\frac{n\pi}{2})(1 - \cos(n\pi))} \cos(n\pi) \tag{17}$$

$$k_2 = \sum_{n=1}^{\infty} \frac{8\,\beta_2}{\lambda_n sin^2(\frac{n\pi}{2})(1 - cos(n\pi))} cos(n\pi) \tag{18}$$

Moreover, k_1 and k_2 for simply supported TBT nanobeam are created as

$$k_1 = \sum_{n=1}^{\infty} \frac{\beta_1}{\lambda_n \Lambda_n \sin^2\, \frac{n\pi}{2}} \tag{19}$$

$$k_2 = \sum_{n=1}^{\infty} \frac{\beta_2}{\lambda_n \Lambda_n\, sin^2\, \frac{n\pi}{2}} \tag{20}$$

Finally, k_1 and k_2 for clamped supported TBT nanobeam are obtained as below

$$k_1 = \sum_{n=1}^{\infty} \alpha_1\, \frac{sin(n\pi)(\frac{2n\pi}{L})}{(1 - cos(n\pi))} \tag{21}$$

$$k_2 = \sum_{n=1}^{\infty} \alpha_2\, \frac{\sin(n\pi)(\frac{2n\pi}{L})}{(1 - \cos(n\pi))} \tag{22}$$

Where $\alpha_1 = \frac{2L(k_sGA)^2B}{\lambda_n \sin\frac{n\pi}{2}\cos\frac{n\pi}{2}[-EI_1\left(\frac{n\pi}{l}\right)^2 - k_sGA]}$ and $\alpha_2 = \frac{2L(k_sGA)^2B}{\lambda_n \sin\frac{n\pi}{2}\cos\frac{n\pi}{2}[-EI_2\left(\frac{n\pi}{l}\right)^2 - k_sGA]}$.

The contact stiffness k_c in Hertz's Law is represented by [6]:

$$k_c = \frac{4}{3}E\sqrt{R} \text{ where } \frac{1}{E} = \frac{1+v_1^2}{E_s} + \frac{1+v_2^2}{E_t},\ \frac{1}{R} = \frac{1}{R_s} + \frac{1}{R_t} \tag{23}$$

Where, E_s and E_t are the elastic moduli, R_s and R_t are the radii of curvature, and v_s and v_t are the Poisson ratios of the striker and target respectively.

FE SIMULATION

The solid element 165 with eight nodes per element is used for simulation of the striker and target in software ANSYS/LSDYNA.

The striker is represented as the spherical Au rigid body with radius 10 Angstroms. The striker velocity is 5 Angstroms/picosecond [13].

In simulations clamped and simply supported boundary conditions with different aspect ratios (length/diameter) are considered.

Therefore the nanotube is considered as the two cylindrical layers model with outer diameter 2.03 nm and inner diameter 1.35 nm so the wall thickness is 2*t*=0.68 nm, Young's modulus *E*=1.06 GPa.

The Schematic of DWCNT with zigzag (21, 0) @ zigzag (21, 0) configuration is represented in Figure 2.

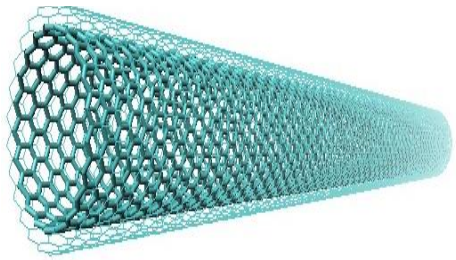
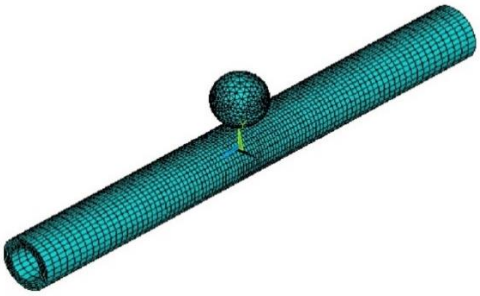


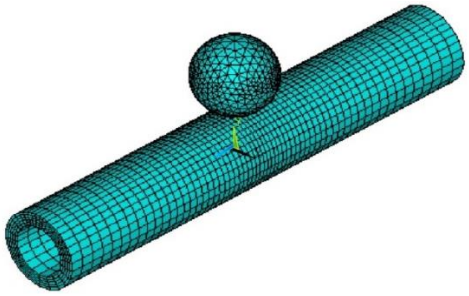
Fig. 2. Schematic of DWCNT with zigzag (21, 0) @ zigzag (21,0) configuration

The FE simulation is done for DWCNT with L/d=2, 4, 6, 8 and 10. The FE mesh model of DWCNT and sphere striker are plotted in Figure 3 for FEM simulation with L/d=8 and 10.



(L/d=10)

(a)

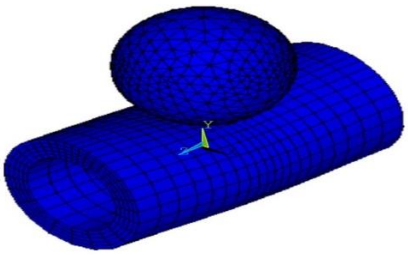


(L/d=8)

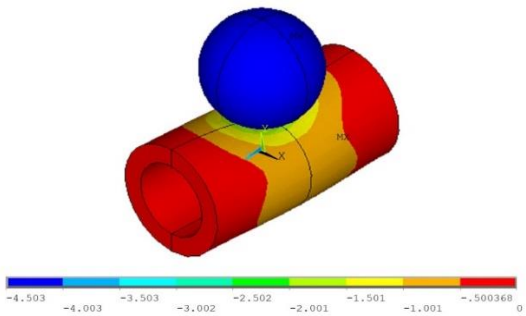
(b)

Fig. 3. The FE mesh of DWCNT and sphere striker with L/d=10 and L/d=8

The deformation shape and displacement Contour of clamped DWCNT with L/d=2 in FEM simulation are plotted in Figures 4(a-b) respectively. As can be seen from Figures 4(a-b), the maximum local deformation occurs in the top center location of DWCNT.



(a)



(b)

Fig. 4. DWCNT with L/d=2,a) The deformation,b) displacement Contour

The comparison between global and local deformation of DWCNT with L/d=10 is shown in Figure 5. The results of FEM simulation are discussed in the result section.

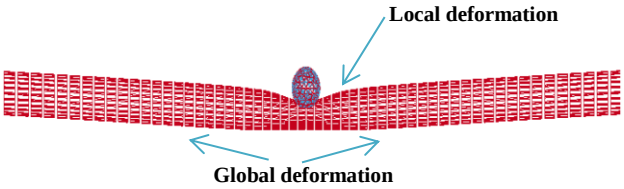


Fig. 5. The local and global deformation shapes of DWCNT and sphere striker with L/d=10

RESULTS AND DISCUSSION

The dimensionless maximum transverse deflection of DWCNT in the analytical model is compared by independent of vdW forces and with considering (depending) the vdW force for different length/diameter of nanotube in Figures (6-7) for simply supported and clamped boundary conditions respectively.

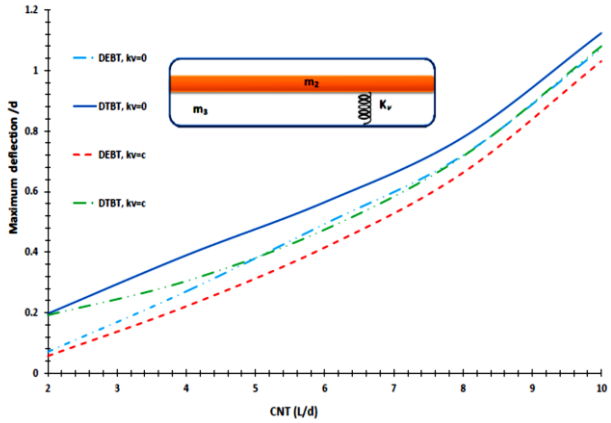


Fig. 6. Effect of van der Waals interaction on dimensionless maximum dynamic deflections of simply supported DWCNT

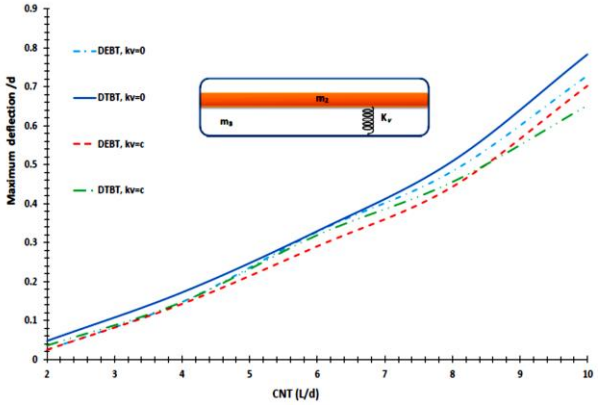


Fig. 7. Effect of van der Waals interaction on dimensionless maximum dynamic deflections of clamped supported DWCNT

It is concluded from Figure 6 and Figure 7 that by including vdW interaction between two layers the maximum deflection is decreased. From these figures indicated that the DWCNT without vdW forces are more flexible than DWCNT with vdW forces. Therefore in the semi-analytical model with the case of $k_v \neq 0$ is having more stiffness in compared with DWCNT without vdW forces.

In other hands the vdW interaction effect makes the DWCNT more flexible as the independent of vdW forces may be viewed as layers linked by elastic springs while the independent model assumes the spring constant to take on an infinite value.

The dimensionless maximum deflections obtained from the semi-analytical model and FE simulations are compared in Figures 8-9 for simply and clamped boundary conditions respectively.

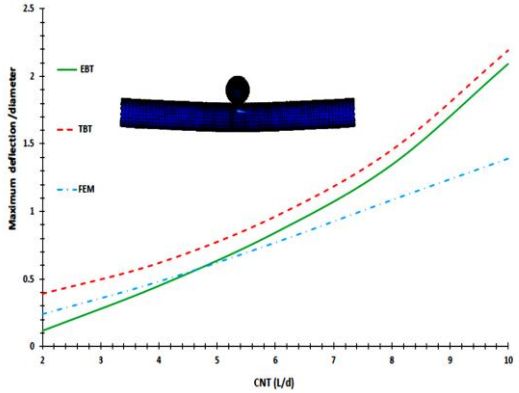


Fig. 8. Dimensionless maximum deflection for analytical EBT and TBT model in comparison with FE simulation with simply boundary condition

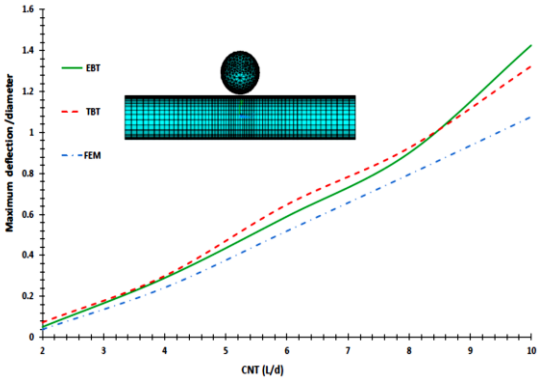


Fig. 9. Dimensionless maximum deflection for analytical EBT and TBT model in comparison with FE simulation with clamped boundary condition

It can be seen from the figures that the FE simulation results without considering the vdW interaction have significant differences with the spring-mass model involving the vdW interaction between the two layers on the value of the maximum deflection of DWCNT. From Figures, it can be seen that the analytical results demonstrated good agreement with FE simulations results.

In the case of the SWCNT, vdW interaction is deleted. In Figures 10-11 the dimensionless maximum deflection for SWCNT and DWCNT are compared for both the simply and clamped supported and by considering the Euler-Bernoulli (SEBT and DEBT) beam and Timoshenko beam (STBT and DTBT).

From Figure 10 and Figure 11, it is clearly seen that the dimensionless maximum deflection of SWCNT is more than DWCNT.

Due to the effects of transverse shear deformation and rotary inertia, the dimensionless maximum deflection of the Timoshenko nanotube model is bigger than the Euler-Bernoulli nanotube model.

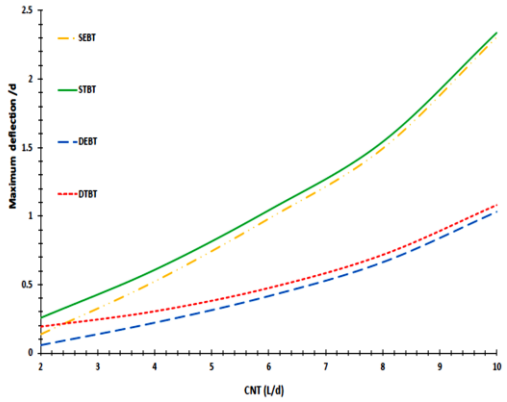


Fig. 10. Dimensionless maximum deflection versus nanotube aspect ratio for SWCNT and DWCNT with simply supported

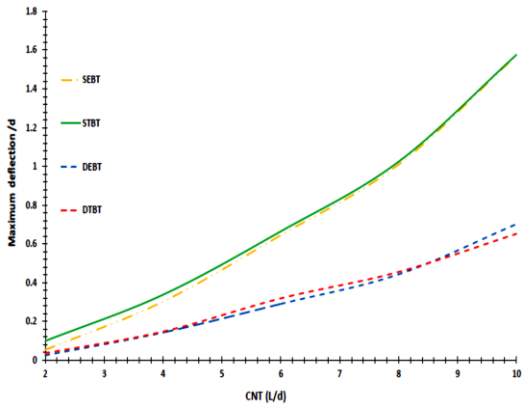


Fig. 11. Dimensionless maximum deflection versus nanotube aspect ratio for SWCNT and DWCNT with clamped supported

The maximum transverse dynamic deflection of simply supported and clamp supported DWCNT for the different velocity of nanoparticle in the analytical model are shown in Figure 12 and 13 respectively.

It is clearly seen from Figures that by increasing the velocity of nanoparticle the maximum dynamic deflection increases.

It is indicated that the deflection of DLGS is not linear due to caused vibration and interaction between the two layers.

Finally, the spherical striker mass influences on deflection results are detected by changing the striker radius.

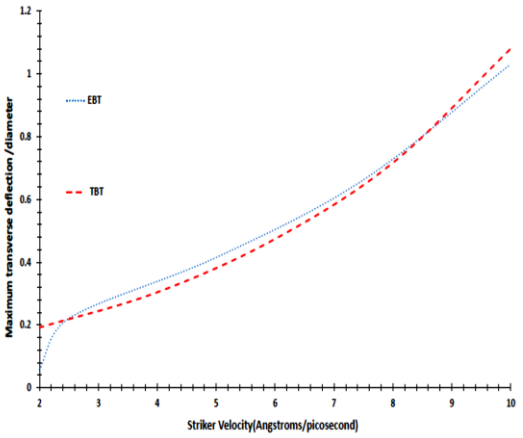


Fig. 12. Dimensionless maximum deflections versus velocity for DWCNT (EBT, TBT) with simply supported

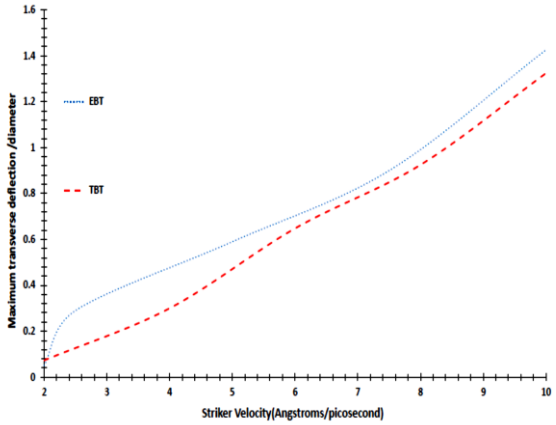


Fig. 13. Dimensionless maximum deflections versus velocity for DWCNT (EBT, TBT) with clamped supported

The semi-analytical deflection results of various striker radii from 5 to 35 Å at the velocity of 5 Å/ps are presented in Figure 14.

This Figure shows that an increase of the mass ratio (striker/nanotube) increases the dimensionless maximum deflection.

By increasing the striker radius more than 16 Å, increasing striker radius will result in a less increase in the dynamic deflection because the stress concentration is more uniform in the contact zone with the increase of the striker radius.

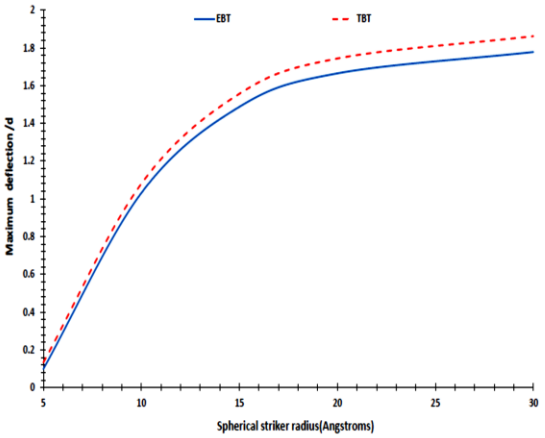


Fig. 14. Dimensionless maximum deflections versus the striker radius for DWCNT

CONCLUSION

In this paper, a new semi-analytical model is obtained to study the impact of a striker on a DWCNT based on the spring-mass system. The vdW interaction between two layers is incorporated. FE simulations were carried out for a series of DWCNT with various values of side-length and striker mass and velocity. It was concluded that the semi-analytical model is a good agreement with FE simulations. Based on the semi-analytical model and FE simulations of impact with different striker velocity and mass, it can be concluded that the maximum dynamic deflection increased with the increase of striker kinetic energy. In addition, at the high mass ratio, the influence of increasing dynamic deflection is decreasing. The DWCNT independent of vdW interaction is more flexible than DWCNT with vdW forces. On the other hand, by considering the vdW force between layers the maximum dynamic deflection of DWCNT is decreased because the stiffness in DWCNT is increased.

REFERENCES

[1] Eringen AC. On differential equations of nonlocal elasticity and solutions of screw dislocation and surface waves. Journal of applied physics. 1983 Sep; 54(9): 4703-10.

[2] Eringen AC. Nonlocal continuum field theories. Springer Science & Business Media; 2002 Jun 14.

[3] Eringen AC, Edelen DG. On nonlocal elasticity. International Journal of Engineering Science. 1972 Mar 1; 10(3): 233-48.

[4] Seifoori S, Liaghat GH. Low Velocity Impact of a Nanoparticle on Euler-Bernoulli Nanobeam using a Nonlocal Elasticity Model. Modares Mechanical Engineering. 2013; 13: 37- 44.

[5] Seifoori S, Liaghat GH, Foladi M. Low velocity impact on Timoshenko nanobeam using a nonlocal elasticity theory. Modares Mechanical Engineering. 2013; 8: 151-160.

[6] Reddy JN. Nonlocal theories for bending, buckling and vibration of beams. International Journal of Engineering Science. 2007 Feb 1; 45(2-8): 288-307.

[7] Reddy JN. Nonlocal nonlinear formulations for bending of classical and shear deformation theories of beams and plates. International Journal of Engineering Science. 2010 Nov 1; 48(11): 1507-18.

[8] Şimşek M. Nonlocal effects in the forced vibration of an elastically connected double-carbon nanotube system under a moving nanoparticle. Computational Materials Science. 2011 May 1; 50(7): 2112-23.

[9] Seifoori S, Liaghat GH. Low velocity impact of a nanoparticle on nanobeams by using a nonlocal elasticity model and explicit finite element modeling. International Journal of Mechanical Sciences. 2013 Apr 1; 69: 85-93.

[10] Seifoori S, Hajabdollahi H. Impact behavior of single-layered graphene sheets based on analytical model and molecular dynamics simulation. Applied Surface Science. 2015 Oct 1; 351: 565-72.

[11] Pradhan SC, Phadikar JK. Nonlocal elasticity theory for vibration of nanoplates. Journal of Sound and Vibration. 2009 Aug 7; 325(1-2): 206-23.

[12] Seifoori S, Khoshgoftar MJ. Impact and vibration response of multi-layered graphene sheets under different striker based on the analytical model and molecular dynamics. Superlattices and Microstructures. 2019 Nov 1; 135: 106249.

[13] Seifoori S, Alibiglo A, Liaghat G, Pol M. Explicit finite element modeling of impact loading on nanobeam to compare with Euler–Bernoulli and Timoshenko theory. Modares Mechanical Engineering. 2015 Jan 1; 14(13).